photonics

MDPI

Communication

Double-Junction Cascaded GaAs-Based Broad-Area Diode Lasers with 132W Continuous Wave Output Power

Jun Wang [1,2,*,†], Shaoyang Tan [1,†], Ye Shao [1], Wuling Liu [2], Kun Tian [1], Yao Xiao [2], Zhicheng Zhang [2], Yudan Gou [2], Lihong Zhu [2], Bangguo Wang [2] and Shouhuan Zhou [2]

1 Suzhou Everbright Photonics Company Ltd., Suzhou 215000, China
2 College of Electronics and Information Engineering, Sichuan University, Chengdu 610065, China
* Correspondence: wjdz@scu.edu.cn
† These authors contributed equally to this paper.

Abstract: Improving the output power and efficiency of broad-area diode lasers is a prerequisite for the further development of fiber lasers, solid-state laser industries, and direct semiconductor laser applications. At present, the large amount of Joule heat generated by large drive currents and limited wall-plug efficiency presents the largest challenge for improving these lasers. In this paper, a multi-junction cascade laser with low Joule heat generation is demonstrated, showing large power and conversion efficiency. We fabricated devices with different junction numbers and compared their output power. We present double-junction lasers emitting at ~915 nm with an emitter width of 500 µm, delivering 132.5 W continuous wave output power at 70 A, which is the highest power reported so far for any single-emitter laser. The power conversion efficiencies are 66.7% and 60%, at 100 W and 132 W, respectively.

Keywords: semiconductor laser; high power; broad-area diode laser; multi-junction

Citation: Wang, J.; Tan, S.; Shao, Y.; Liu, W.; Tian, K.; Xiao, Y.; Zhang, Z.; Gou, Y.; Zhu, L.; Wang, B.; et al. Double-Junction Cascaded GaAs-Based Broad-Area Diode Lasers with 132W Continuous Wave Output Power. *Photonics* **2024**, *11*, 258. https://doi.org/10.3390/photonics11030258

Received: 11 February 2024
Revised: 25 February 2024
Accepted: 12 March 2024
Published: 13 March 2024

1. Introduction

High-power broad-area laser diodes (HP-BALs) have emerged as primary pump sources for fiber and solid-state laser systems for diverse industrial applications, owing to their large power conversion efficiency (PCE), reliability, and cost-effectiveness [1–17]. In the dynamic landscape of fiber lasers and solid-state lasers, there is an increasing demand for such lasers, capable of delivering even larger output power and PCE.

In the last 20 years, breakthroughs in terms of both power and efficiency have been reported [7–13]. In 2008, Petrescu-Prahova et al. demonstrated BALs with 100 µm emitter width, operating at room temperature, and achieving an output power of 25.3 W from both facets [14]. Subsequently, in 2017, V. Gapontsev et al. reported a BAL with output power exceeding 30 W [15]. In 2022, Yuxian Liu et al. advanced the output power, ultimately reaching 48 W [16]. In 2023, we presented BALs with a width of 230 µm, operating at room temperature, delivering an impressive 51 W output power [17]. The significant progress presented hitherto in this paper have been confirmed to be based on more detailed analyses than the sources of power and efficiency limitations.

With an increasing drive current, all lasers first show a saturation and then a reduction in quantum efficiency. The Joule heat, generated upon increasing injection currents, raises the temperature of the active area, broadens the gain, and decreases the peak gain, thus limiting the output power. Our approach involves stacking multiple epitaxial layers using tunneling junction technology developed by us, which eventually lead to an enormous shift of the present limits [18]. In comparison to traditional devices, multi-junction devices can achieve larger output power at lower current levels and reduced Joule heat. Presently, tunnel junction technology has already achieved breakthroughs and found wide-spread application in short-pulse Vertical Cavity Surface Emission Lasers (VCSELs) and Light Detection and Ranging (LiDAR) systems [19–23]. Applications of tunnel junctions for continuous-wave (CW) operation lasers have been limited so far due to challenges such as thermal accumulation, difficulties in the control of the lateral optical field, multi-junction failure, and difficulties in coupling into optical fibers. Recent reports on tunnel junction cascade technology in the context of CW operation lasers have been relatively scarce.

In this paper, we present a comprehensive analysis of double-junction GaAs-based broad-area diode lasers (double-junction BALs), specifically highlighting their capability to achieve room temperature CW ultra-high laser output power, at unprecedented levels. An electro-optical simulation and design study of double-junction BALs is conducted. The simulations reveal that at room temperature, double-junction BALs result in reduced Joule heat generation at equivalent output power levels. The thermal simulation results show that the double-junction structure does not significantly affect the heat dissipation in the device. Concurrently, we fabricated high-power BALs, incorporating varying junctions based on a single-junction device with low internal loss and thermal stability, and meticulously compared their output characteristics. Experimental results demonstrate that double-junction high-power BALs emit a record CW output power of up to 132.5 W at room temperature. Moreover, the corresponding power conversion efficiency still maintains 60%, with a peak efficiency near 70%. The optical power density at the output mirror of these BALs is 50% compared to single-junction BALs, significantly enhancing device reliability.

2. Simulation and Design

In Figure 1a, we illustrate the epitaxially stacked double-junction structure, consisting of two laser heterostructures connected by a GaAs tunnel junction (TJ) [22]. The main layer structure of the double junctions, including the active region, waveguide layer, and cladding layer, is identical. The main layer structure of the double junctions comprises an asymmetric large optical cavity structure, consisting of a single InGaAs/AlGaAs quantum well sandwiched in a AlGaAs waveguide, an n-type AlGaAs cladding, and a p-type AlGaAs cladding. To clearly illustrate the structure details, Figure 1b depicts the refractive index profile, along with the fundamental mode profile of the single-junction BAL in the vertical direction, as calculated in the following section. The emitter width is 500 μm, and the cavity length is 5.6 mm, respectively. The facet reflectivity is 1.5% and 99% for the front and rear facets, respectively. Our simulations are built using Crosslight software with a 1D carrier and optical model, excluding thermal effects. The simulation model is calibrated using experimental data from single-junction BALs at room temperature. We calculate the L-I-V characteristics, output power, conversion efficiency, and temperature dependence of single- and double-junction laser structures. It is important to note that for the simulations, we assumed constant internal quantum efficiency. The simulation results are shown in Figure 2. Figure 2a shows that the output power increases as the number of junctions increases if the emitter width is kept constant. Assuming adequate heat sink capacity, the injection current producing 132 W output power decreases from 130.2 A of a single-junction BAL to 60.8 A of a double-junction BAL. The effect of junction number on BALs' heat dissipation was evaluated by solving the steady-state heat conduction equation using the finite elements method. Figure 2d shows that with the increase in thermal power, the temperature in the active regions gradually increases. Since the double junctions are vertically cascaded in the epitaxial layer, each junction will have a different temperature due to its different distances from the heat sink. The active region farthest away from the heat sink has the highest temperature.

We fabricated single-junction and double-junction BALs. Double heterostructures were grown on n-type 6″ GaAs substrates by metalorganic chemical vapor deposition (MOCVD) using an asymmetric large optical cavity structure. Each active region comprises a single compressively strained InGaAs/AlGaAs quantum well (QW) optimized for efficient emission at a wavelength near 915 nm. Following epitaxial growth, a 500 μm wide mesa was patterned using conventional lithography and wet etching. Subsequently, the contact window of the SiO_2 insulation layer was opened, and the p-metal contact was deposited. The substrate was then thinned, followed by N-metallization. Ultimately, single-emitter laser chips with a cavity length of 5.6 mm were cleaved. The front and back facets were passivated and coated with anti-reflective (AR) and high-reflective (HR) coatings, respectively. The chips were bonded p-side down on a diamond substrate using indium solder.

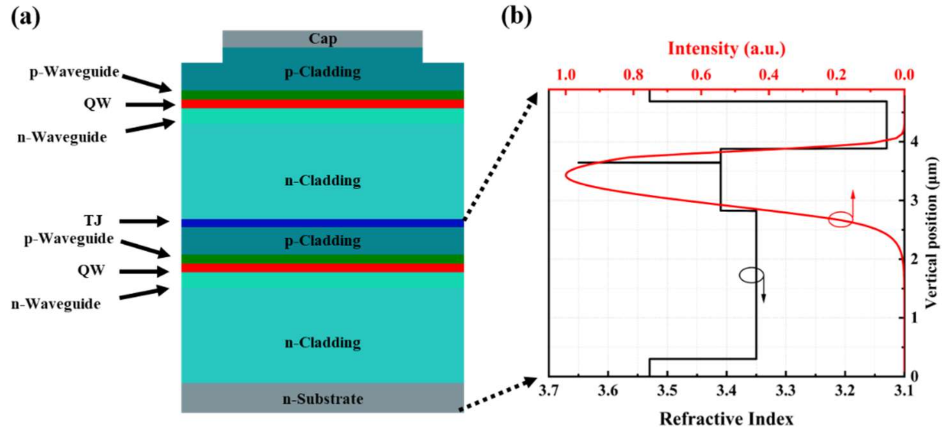

Figure 1. (**a**) Schematic diagram of the 2-junction BAL structure, including substrate, cladding layer, waveguide layer, cap, quantum well (QW), and tunnel junction (TJ). (**b**) Profiles of refractive index and calculated intensity of the fundamental vertical mode of single-junction BAL.

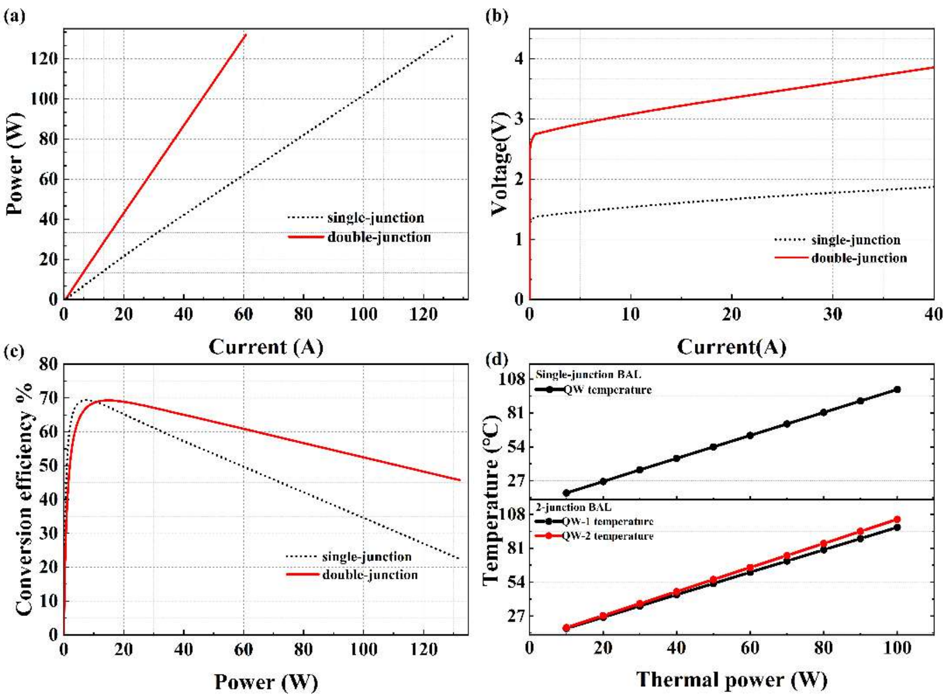

Figure 2. Numerical simulation of the output characteristics of the BAL with a single and a double junction. (**a**) With the increase in the number of junctions, the drive current required decreases linearly for the same output power. (**b**) As the number of junctions increases, the opening voltage of the BAL also increases linearly. (**c**) The PCE peak moves slightly to higher power with the increase in the number of junctions. For larger power, the double-junction device has an increased PCE. (**d**) Temperature of the active region versus thermal power for BAL for different junction numbers.

3. Results and Discussion

Figure 3 shows cross-section scanning electron microscopy (SEM) images of single-junction and double-junction BALs prepared by focused ion beam (FIB) etching. The L-I-V results of BALs with varying junction numbers are depicted in Figure 4a,b. It is evident that, with increasing current, the output power increases almost linearly, and no thermal roll-over is observed within the present current range. As illustrated in Figure 4a, the threshold of the single-junction BAL was 3.5 A, while that of the double-junction BAL was 3.4 A, showing little difference. The slope efficiency and threshold voltage of the BAL increased proportionally with the number of p–n junctions. The slope efficiency of the double-junction BAL reached 2.30 W/A and the threshold voltage exceeded 2.6 V. The large threshold voltage and lower current for identical output power are very advantageous since lower current implies reduced Joule heating. Consequently, at large current injections (threshold current proportion becomes quite small and the effect on optical power can be neglected), the Joule heating of the double-junction device can be reduced to 50%, resulting in larger output power. Figure 4a shows that for a specified power of 81 W, the max output power of a single-junction LD is achieved, and the Joule heat created for single-junction and double-junction devices is 47.9 W and 36.2 W, respectively, corresponding to 37% and 31.4% of the injected power. Concurrently, the optical power density of the double-junction device is merely 0.081 W/μm, half that of the single-junction device, thereby significantly improving the reliability of the device. Notably, the peak power of the double-junction BAL exceeds 132.5 W at a current of 70 A, for a heat sink temperature maintained at 25 °C. To the best of the authors' knowledge, this is the largest output power value for single-emitter BALs so far. Figure 4b illustrates that for increasing the number of junctions, the double-junction device exhibits higher PCE for larger output power, particularly away from the threshold, being 66.7% and 60% at 100 W and 132 W, respectively, although the peak PCE decreased slightly from 71.8% to 69.3%.

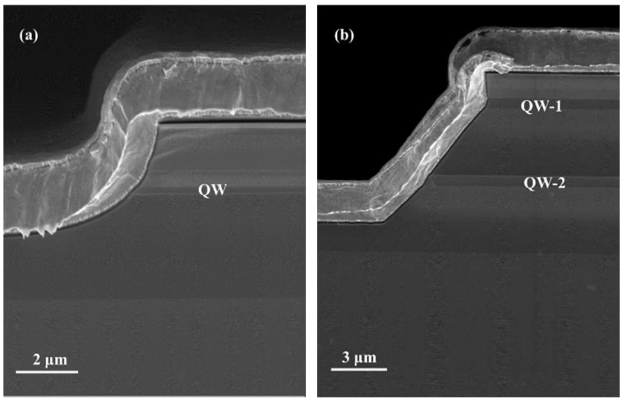

Figure 3. Cross-section SEM image of the (**a**) single-junction BAL and (**b**) double-junction BAL.

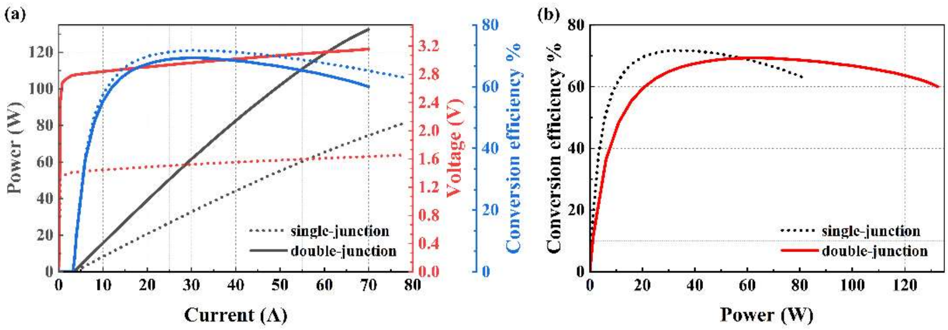

Figure 4. (**a**) L-I-V results of BALs with different junction numbers. The output power of the double-junction BAL exceeds 132.5 W at a current of 70 A and a heat sink temperature of 25 °C. black line: power; blue line: conversion efficiency; red line: voltage (**b**) PCE versus output power for BALs with different junction numbers.

The temperature characteristics of the device were assessed using the spectral drift method [24], employing a spectral drift coefficient of 0.32 nm/K. In Figure 5a, the temperatures of single- and double-junction devices are presented as a function of output power. For output power below 48 W, the single-junction device exhibits a lower temperature.

However, as the output power increases, the temperature rises rapidly. In contrast, the double-junction device is advantageous at larger currents, in agreement with our simulations. For an output power of 132.5 W for the single-junction device, the device temperature is 89 °C, which is 30 °C higher than that of the double-junction device. Larger junction temperatures lead to reduced internal quantum efficiency and increased internal losses. Consequently, optical power gradually saturates, as indicated by the L–I curve presented in Figure 4a. Figure 5b shows the emission spectra of the double-junction BAL as a function of injection current, revealing a notable broadening of the spectra, particularly evident at injection currents of 60 A and 70 A. This observation is attributed to the different distances of the two QWs from the heat sink, resulting in a marginally higher temperature of QW-2 compared to QW-1, and a broadening of the Fermi distribution of the carriers in the QWs. Spectral analysis revealed a 1.35 nm difference in peak wavelength between the two active regions at 70 A current, corresponding to a temperature difference of approximately 4.2 °C, consistent with our simulations. The spectrum broadening can be suppressed by a blue shift of the gain peak in epitaxy process.

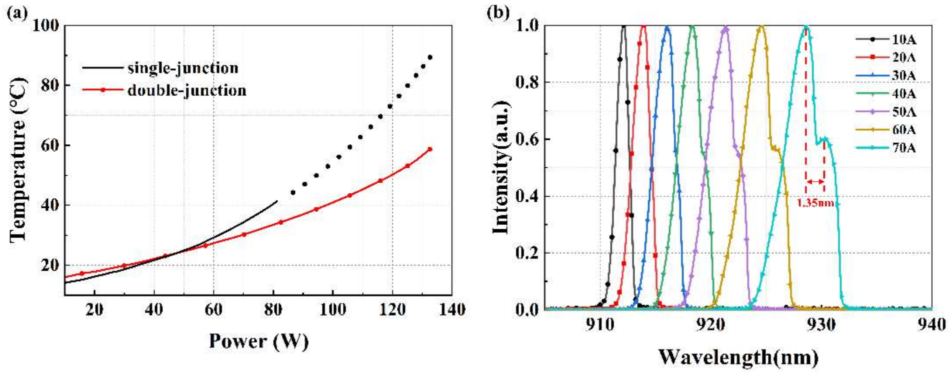

Figure 5. (**a**) Output temperature vs. output power of BALs with different junction numbers. The double-junction device has a lower temperature than the single-junction device. (**b**) Emission spectra of double-junction BAL at different driving currents.

Figure 6a shows the near-field profile of the double-junction BAL, as obtained through the slit-scan method at a 61 A injection current. The near-field profile appears uniformly spread, with a width of approximately 491.5 µm, encompassing 95% of the power. The near-field CCD image and the optical microscope photograph of the cavity facet demonstrate that the near-field width is almost identical to the current injection width. Although there is a subtle expansion of the current in QW-2, it does not extend to the edge of the groove. This observation proves that the current spread resulting from the tunnel junction is negligible. In Figure 6b, the lateral and transverse far-field profiles under the 61 A injection current are depicted. The lateral far-field divergence angle, encompassing 95% of the power, is approximately 12.4°, while the transverse far-field divergence angle is around 51°.

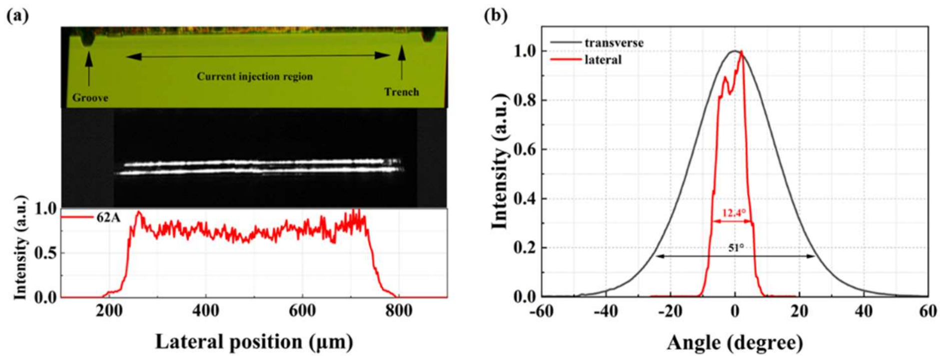

Figure 6. (**a**) Near−field CCD image and lateral intensity profile at 62 A, as well as microscope image of the emitting facet. (**b**) Lateral far-field profile and transverse far-field profile of 62 A.

4. Conclusions

We compared the output characteristics of single- and double-junction BALs. Simulations indicate that double-junction BALs exhibit lower injection currents, resulting in reduced Joule heat generation at equivalent output power levels at room temperature. Consequently, multi-junction BALs offer a novel approach to increase the power output of BALs. To validate this assertion, we fabricated BALs as simulated and conducted a comprehensive analysis of their output characteristics. Encouragingly, our data reveal that the double-junction BAL achieves an optical power output of 132.5 W at a heat sink temperature of 25 °C under CW conditions. The power conversion efficiency is 66.7% and 60% at 100 W and 132 W, respectively. The optical power density is only half of that of single-junction BALs, markedly enhancing the reliability of double-junction BALs. To the best of our knowledge, our results represent the largest ever reported single-emitting CW power in the field of semiconductor lasers.

Author Contributions: Conceptualization, J.W. and S.T.; Data curation, Y.S., W.L. and K.T.; Formal analysis, Y.S. and W.L.; Investigation, Y.X., Z.Z., Y.G., L.Z. and B.W.; Methodology, J.W. and S.T.; Project administration, J.W.; Resources, J.W. and S.Z.; Supervision, J.W. and S.T.; Writing—original draft, W.L.; Writing—review and editing, J.W. and S.T. All authors have read and agreed to the published version of the manuscript.

Funding: This research received no external funding.

Data Availability Statement: The data presented in this study are available on reasonable request from the corresponding author.

Conflicts of Interest: Authors Jun Wang, Shaoyang Tan, Ye Shao and Kun Tian were employed by the company Suzhou Everbright Photonics Company Ltd. The remaining authors declare that the research was conducted in the absence of any commercial or financial relationships that could be construed as a potential conflict of interest.

References

1. Leisher, P.O.; Labrecque, M.; McClune, K.; Burke, E.; Renner, D.; Campbell, J. Origin of the longitudinal current crowding effect in high power diode lasers. In Proceedings of the 2021 27th International Semiconductor Laser Conference (ISLC), Potsdam, Germany, 10–14 October 2021; IEEE: New York, NY, USA, 2021; pp. 1–2.
2. Arslan, S.; Wenzel, H.; Fricke, J.; Thies, A.; Ginolas, A.; Eppich, B.; Tränkle, G.; Crump, P. Experimental and theoretical studies into longitudinal spatial hole burning as a power limit in high-power diode lasers at 975 nm. *Appl. Phys. Lett.* **2023**, *122*, 261101. [CrossRef]
3. Arslan, S.; Swertfeger, R.B.; Fricke, J.; Ginolas, A.; Stölmacker, C.; Wenzel, H.; Crump, P.A.; Patra, S.K.; Deri, R.J.; Boisselle, M.C. Non-uniform longitudinal current density induced power saturation in GaAs-based high power diode lasers. *Appl. Phys. Lett.* **2020**, *117*, 203506. [CrossRef]
4. Todt, R.; Deubert, S.; Jaeggi, D. High-volume manufacturing of state-of-the-art high-power laser diodes on 6-inch GaAs. In Proceedings of the High-Power Diode Laser Technology XX, San Francisco, CA, USA, 22 January–28 February 2022; SPIE: Bellingham, WA, USA, 2022; Volume 11983, pp. 11–19.
5. Wang, J.; Smith, B.; Xie, X.; Wang, X.; Burnham, G.T. High-efficiency diode lasers at high output power. *Appl. Phys. Lett.* **1999**, *74*, 1525–1527. [CrossRef]
6. Miah, M.J.; Strohmaier, S.; Urban, G.; Bimberg, D. Beam quality improvement of high-power semiconductor lasers using laterally inhomogeneous waveguides. *Appl. Phys. Lett.* **2018**, *113*, 221107. [CrossRef]
7. Boni, A.; Arslan, S.; Erbert, G.; Della Casa, P.; Martin, D.; Crump, P. Epitaxial design progress for high power, efficiency, and brightness in 970 nm broad area lasers. In Proceedings of the High-Power Diode Laser Technology XIX, Online, 6–12 March 2021; SPIE: Bellingham, WA, USA, 2021; Volume 11668, pp. 15–22.
8. Campbell, J.; Labrecque, M.; Foong, F.; Renner, D.; Mashanovitch, M.; Leisher, P. Watt-class, COMD-free ridge waveguide lasers at 885 nm. In Proceedings of the 2021 27th International Semiconductor Laser Conference (ISLC), Potsdam, Germany, 10–14 October 2021; IEEE: New York, NY, USA, 2021; pp. 1–2.
9. Crump, P.; Elattar, M.; Miah, M.J.; Ekterai, M.; Karow, M.M.; Martin, D.; Della Casa, P.; Maaßdorf, A.; McDougall, S.; Holly, C.; et al. Progress in experimental studies into the beam parameter product of GaAs-based high-power diode lasers. In Proceedings of the High-Power Diode Laser Technology XX, San Francisco, CA, USA, 22 January–28 February 2022; SPIE: Bellingham, WA, USA, 2022; Volume 11983, pp. 43–52.

10. King, B.; Arslan, S.; Boni, A.; Basler, P.S.; Zink, C.; Della Casa, P.; Martin, D.; Thies, A.; Knigge, A.; Crump, P. GaAs-based wide-aperture single emitters with 68 W output power at 69% efficiency realized using a periodic buried-regrown-implant-structure. In Proceedings of the the European Conference on Lasers and Electro-Optics, Munich, Germany, 26–30 June 2023; Optica Publishing Group: Washington, DC, USA, 2023; p. cb_11_1.
11. Wang, B.; Tan, S.; Zhou, L.; Zhang, Z.; Xiao, Y.; Liu, W.; Gou, Y.; Deng, G.; Wang, J. High Reliability 808nm Laser Diodes with Output Power Over 19W Under CW Operation. *IEEE Photonics Technol. Lett.* **2022**, *34*, 349–352. [CrossRef]
12. Miah, M.J.; Boni, A.; Martin, D.; Della Casa, P.; Crump, P. Highly asymmetric epitaxial designs for increased power and efficiency in kW-class gaas-based diode laser bars. In Proceedings of the 2021 27th International Semiconductor Laser Conference (ISLC), Potsdam, Germany, 10–14 October 2021; IEEE: New York, NY, USA, 2021; pp. 1–2.
13. Crump, P.; Grimshaw, M.; Wang, J.; Dong, W.; Zhang, S.; Das, S.; Farmer, J.; DeVito, M.; Meng, L.S.; Brasseur, J.K.; et al. 85% power conversion efficiency 975-nm broad area diode lasers at −50 C, 76% at 10 C. In Proceedings of the 2006 Conference on Lasers and Electro-Optics and 2006 Quantum Electronics and Laser Science Conference, Long Beach, CA, USA, 21–26 May 2006; IEEE: New York, NY, USA, 2006; pp. 1–2.
14. Petrescu-Prahova, I.B.; Modak, P.; Goutain, E.; Bambrick, D.; Silan, D.; Riordan, J.; Moritz, T.; Marsh, J.H. 253 mW/μm maximum power density from 9xx nm epitaxial laser structures with d/Γ greater than 1 μm. In Proceedings of the 2008 IEEE 21st International Semiconductor Laser Conference, Sorrento, Italy, 14–18 September 2008; IEEE: New York, NY, USA, 2008; pp. 135–136.
15. Gapontsev, V.; Moshegov, N.; Berezin, I.; Komissarov, A.; Trubenko, P.; Miftakhutdinov, D.; Berishev, I.; Chuyanov, V.; Raisky, O.; Ovtchinnikov, A. Highly-efficient high-power pumps for fiber lasers. In Proceedings of the High-Power Diode Laser Technology XV, San Francisco, CA, USA, 28 January–2 February 2017; SPIE: Bellingham, WA, USA, 2017; Volume 10086, pp. 16–25.
16. Liu, Y.; Yang, G.; Zhao, Y.; Tang, S.; Lan, Y.; Zhao, Y.; Demir, A. 48 W continuous-wave output from a high-efficiency single emitter laser diode at 915 nm. *IEEE Photonics Technol. Lett.* **2022**, *34*, 1218–1221. [CrossRef]
17. Tan, S.; Liu, W.; Wang, B.; Zhao, W.; Wang, J. Lateral brightness improvement of high-power semiconductor laser diode. In Proceedings of the High-Power Diode Laser Technology XXI, San Francisco, CA, USA, 28 January–3 February 2023; SPIE: Bellingham, WA, USA, 2023; Volume 12403, pp. 223–228.
18. Gou, Y.; Wang, H.; Wang, J.; Yang, H.; Deng, G. High performance p++-AlGaAs/n++-InGaP tunnel junctions for ultra-high concentration photovoltaics. *Opt. Express* **2022**, *30*, 23763–23770. [CrossRef] [PubMed]
19. Aboujja, S.; Chu, D.; Bean, D. 1550nm triple junction laser diode for long range LiDAR. In Proceedings of the High-Power Diode Laser Technology XX, San Francisco, CA, USA, 22 January–28 February 2022; SPIE: Bellingham, WA, USA, 2022; Volume 11983, pp. 196–207.
20. Ammouri, N.; Christopher, H.; Maassdorf, A.; Fricke, J.; Ginolas, A.; Liero, A.; Wenzel, H.; Knigge, A.; Traenkle, G. Distributed feedback broad area lasers with multiple epitaxially stacked active regions and tunnel junctions. *Opt. Lett.* **2023**, *48*, 6520–6523. [CrossRef] [PubMed]
21. Choi, A.; Park, J.; Lee, J.; Kim, Y.; Kim, T. 905nm 140W pulse laser diode with 4Stack epitaxy structure for autonomous lidar. In Proceedings of the High-Power Diode Laser Technology XXI, San Francisco, CA, USA, 28 January–3 February 2023; SPIE: Bellingham, WA, USA, 2023; Volume 12403, pp. 37–43.
22. Wenzel, H.; Maaßdorf, A.; Zink, C.; Martin, D.; Weyers, M.; Knigge, A. Novel 900 nm diode lasers with epitaxially stacked multiple active regions and tunnel junctions. *Electron. Lett.* **2021**, *57*, 445–447. [CrossRef]
23. Xiao, Y.; Wang, J.; Liu, H.; Miao, P.; Gou, Y.; Zhang, Z.; Deng, G.; Zhou, S. Multi-junction cascaded vertical-cavity surface-emitting laser with a high power conversion efficiency of 74%. *Light. Sci. Appl.* **2024**, *13*, 60. [CrossRef] [PubMed]
24. Siegal, B. Laser diode junction temperature measurement alternatives: An overview. In Proceedings of the PhoPack, Stanford, CA, USA, 14–16 July 2002.